Physics and polarization characteristics of 298 nm AlN-delta-GaN quantum well ultraviolet light-emitting diodes

Cheng Liu, Yu Kee Ooi, S. M. Islam, Jai Verma, Huili (Grace) Xing, Debdeep Jena, and Jing Zhang

Citation: Appl. Phys. Lett. **110**, 071103 (2017);
View online: https://doi.org/10.1063/1.4976203
View Table of Contents: http://aip.scitation.org/toc/apl/110/7
Published by the American Institute of Physics

Physics and polarization characteristics of 298 nm AlN-delta-GaN quantum well ultraviolet light-emitting diodes

Cheng Liu,[1,a)] Yu Kee Ooi,[1] S. M. Islam,[2] Jai Verma,[3,b)] Huili (Grace) Xing,[2,3,4] Debdeep Jena,[2,3,4] and Jing Zhang[1,5,c)]

[1]*Microsystems Engineering, Rochester Institute of Technology, Rochester, New York 14623, USA*
[2]*School of Electrical and Computer Engineering, Cornell University, Ithaca, New York 14853, USA*
[3]*Department of Electrical Engineering, University of Notre Dame, Notre Dame, Indiana 46556, USA*
[4]*Department of Materials Science and Engineering, Cornell University, Ithaca, New York 14853, USA*
[5]*Department of Electrical and Microelectronic Engineering, Rochester Institute of Technology, Rochester, New York 14623, USA*

(Received 16 November 2016; accepted 31 January 2017; published online 13 February 2017)

This work investigates the physics and polarization characteristics of 298 nm AlN-delta-GaN quantum well (QW) ultraviolet (UV) light-emitting diodes (LEDs). The physics analysis shows that the use of the AlN-delta-GaN QW structure can ensure dominant conduction band (C) to heavy-hole (HH) subband transition and significantly improve the electron and top HH subband wave function overlap. As a result, up to 30-times enhancement in the transverse-electric (TE)-polarized spontaneous emission rate of the proposed structure can be obtained as compared to a conventional AlGaN QW structure. The polarization properties of molecular beam epitaxy-grown AlN/GaN QW-like UV LEDs, which consist of 3–4 monolayer (QW-like) delta-GaN layers sandwiched by 2.5-nm AlN sub-QW layers, are investigated in this study. The polarization-dependent electroluminescence measurement results are consistent with the theoretical analysis. Specifically, the TE-polarized emission intensity is measured to be much larger than the transverse-magnetic emission, indicating significant potential for our proposed QW structure for high-efficiency TE-polarized mid-UV LEDs. *Published by AIP Publishing*. [http://dx.doi.org/10.1063/1.4976203]

Semiconductor ultraviolet (UV) light-emitting diodes (LEDs) and laser diodes (LDs) as potential substitutes for traditional bulky mercury lamps and excimer lasers have attracted substantial interests for numerous applications such as water purification, free space communication, and optical storage.[1–4] Because of their compact size, robust material properties, and long lifetimes, semiconductor UV LEDs could unlock many applications such as UV point sources and highly sensitive UV detectors. Conventionally, AlGaN quantum well (QW) structures are widely utilized as active regions for mid- and deep-UV LEDs.[5–17] Nevertheless, the external quantum efficiencies (η_{EQE}) of AlGaN-based UV LEDs still remain less than 10% for wavelength (λ) < 300 nm till recently.[4–9] This extremely low η_{EQE} can mainly be attributed to the material challenges including high dislocation densities (10^{10} cm^{-2} in AlN and AlGaN layers)[10,11] and relatively low electrical conductivity in p- and n-type AlGaN cladding layers,[12–17] as well as the physics challenges such as a severe valence band-mixing effect in conventional AlGaN QW structures.[18–22]

Specifically, previous studies revealed that the crystal-field split-off (CH) subband is dominant in the valence band for high Al-content (>68%) AlGaN QWs, which results in dominant transverse-magnetic (TM)-polarized emission at $\lambda \sim 220$–230 nm.[18] However, with the decrease in the Al-content, the heavy hole (HH) subband gradually moves toward the highest energy level in the valence band and causes the corresponding transition from the conduction band to the heavy hole subband (C-HH) to mix with C-light hole (LH) and C-CH transitions at $\lambda \sim 250$–300 nm. Consequently, a higher TE-polarized spontaneous emission rate than that of the TM-polarized component is obtained. But both TE- and TM-polarized components have relatively low values in this wavelength regime due to two reasons: (1) the three degenerate valence subbands are closely separated, and thus there is insufficient carrier population in the top HH subband and (2) there is a large spatial separation between the electron and HH wavefunctions, which leads to a small wavefunction overlap. Therefore, it is challenging to realize high-efficiency and high-power mid-UV emitters based on conventional AlGaN QW structures.

To enhance the TE-polarized emission of UV LEDs at $\lambda \sim 250$–300 nm, an active region design with the AlGaN-delta-GaN QW has been proposed previously to substitute the conventional AlGaN-based QW structures.[23] From the theoretical analysis in this previous work, the advantages of inserting the delta-GaN layer in the active region are twofold: (1) the insertion of the GaN layer into the high Al-content AlGaN QW could introduce a strong valence band mixing effect that helps to flip the HH subband back to the highest energy level, which can lead to large TE-polarized emission at $\lambda \sim 250$–300 nm; (2) the thin GaN layer could strongly localize the electron and hole wave functions toward the QW center that leads to significantly improved electron-hole wave function overlap. Nonetheless, considering the epitaxy challenges of growing the AlGaN-delta-GaN QW active region on the AlN substrate, an alternative approach would be the use of an AlN sub-QW layer in replacing the high Al-content

[a)]Electronic mail: cl7007@rit.edu
[b)]Present address: Intel Corporation, Hillsboro, Oregon 97124, USA.
[c)]Electronic mail: Jing.Zhang@rit.edu

AlGaN sub-QW in the AlGaN-delta-GaN QW structure for a much straightforward epitaxy growth (Figure 1(a)). Recent experimental works have reported mid- and deep-UV emission by AlN/GaN superlattices[24] and AlN/GaN quantum dots (QDs).[14–17] However, the exploration of the underlying physics and polarization-dependent optical properties of such an active region, which are essential for improving the performance of such UV emitters, is still relatively lacking.

Therefore, this work investigates the physics and optical properties of AlN-delta-GaN QW structures emitting at 298 nm by employing band structure calculations and polarization-dependent electroluminescence (EL) measurements. Specifically, the band structure and wave function calculations in this study are based on the 6-band $\boldsymbol{k}\cdot\boldsymbol{p}$ model, taking into account the self-consistency, strain effect, polarization electric field, and carrier screening effects.[23,25–28] All the material parameters are taken from Ref. 28. Polarization-dependent EL measurements were performed on the molecular beam epitaxy (MBE)-grown AlN/GaN QW-like UV LEDs. The MBE growth details of the AlN/GaN QW-like active region can be found from Refs. 14–16. From our physics analysis, the insertion of the delta-GaN layer into the AlN sub-QW region could strongly localize the electron and HH wave functions toward the center of the QW, resulting in 30-times enhancement in the TE-polarized spontaneous emission rate at 298 nm as compared to the use of the conventional $Al_{0.35}Ga_{0.65}N$ QW. The EL measurements on an AlN/GaN QW-like UV LED with 3–4 monolayers (MLs) GaN on the AlN/sapphire substrate showed dominant TE-polarized emission for the proposed structure, which again verified our theoretical prediction.

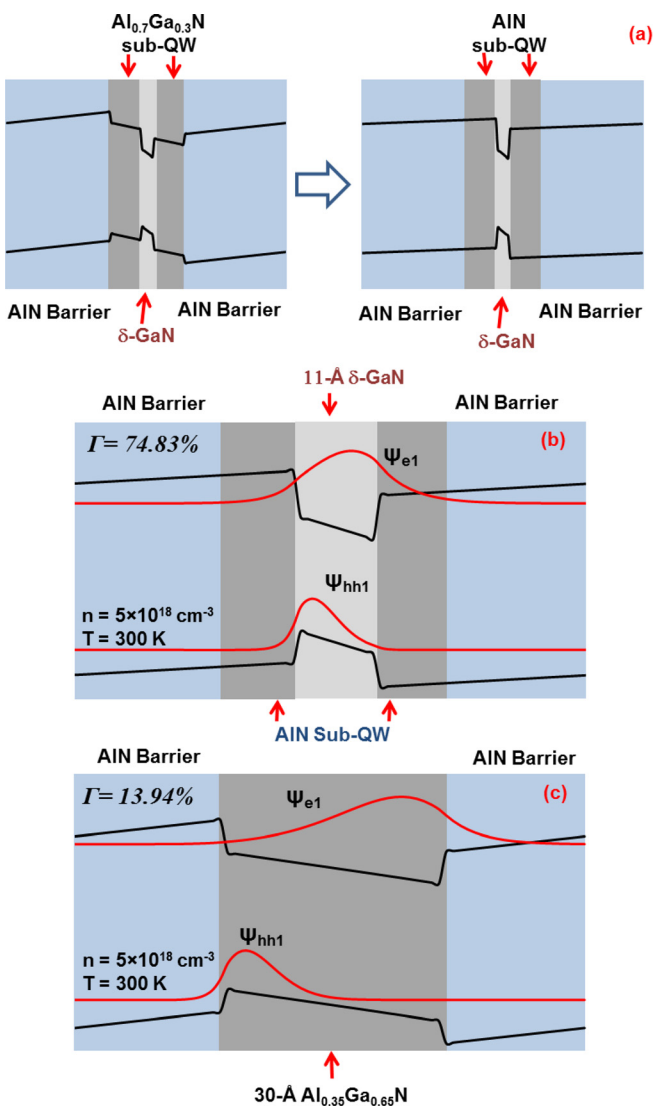

FIG. 1. (a) Band structure transitioned from the $Al_{0.7}Ga_{0.3}N$-delta-GaN QW to the AlN-delta-GaN QW, showing that the use of the AlN sub-QW layer is to replace the AlGaN sub-QW region; Energy band lineups for the (b) AlN-delta-GaN QW; (c) 30-Å conventional $Al_{0.35}Ga_{0.65}N$ QW with ground state electron wave function (ψ_{e1}), heavy hole wave function (ψ_{hh1}), and electron and hole wave function overlap (Γ).

As discussed earlier, Figure 1(a) illustrates the AlN-delta-GaN QW structure with a 2 nm AlN sub-QW region with a 11-Å delta-GaN layer inserted between AlN barriers, which is similar to the MBE-grown AlN/GaN QW-like LED structure. Note that for the AlGaN-delta-GaN QW design, a large Al-content is required to achieve large TE-polarized emission at UV wavelengths. Thus, here we propose to use AlN to serve as the sub-QW region instead of the AlGaN sub-QWs. The design of the proposed AlN-delta-GaN QW structure shows two advantages: (1) the insertion of the delta-GaN structure is to localize the electron and hole wave functions toward the delta-QW center, which ensures a large TE-polarized spontaneous emission rate based on Fermi's golden rule; (2) the use of the AlN-delta-GaN QW together with AlN barriers is a more straightforward process for MBE epitaxy growth as compared to the AlGaN-delta-GaN QW.

Figure 1(b) plots the energy band lineup profiles and wave function of the ground state conduction subband (C1) and the topmost valence subband wave function (HH1) at zone center for the proposed AlN-delta-GaN QW structure. Thus, a dominant TE-polarized spontaneous emission would be expected from this dominant C-HH transition. Note that the delta-GaN that is inserted into the AlN sub-QW region serves as a delta layer instead of a GaN single QW, as the wavefunctions are extended into all the three sub-QW layers as shown in Figure 1(b). As a comparison with similar wavelength, the band structure and wave functions for the conventional 30-Å $Al_{0.35}Ga_{0.65}N$ QW are also shown in Figure 1(c). The Al-content is selected to achieve similar emission wavelength with the proposed structure for carrier density (n) of $5\times10^{18}\,cm^{-3}$ at 300 K. For the conventional $Al_{0.35}Ga_{0.65}N$ QW, large separation between electron and hole wave functions is observed due to the large internal electrostatic field, which results in a very low electron-hole wave function overlap ($\Gamma_{e\_hh}=13.94\%$). In contrast, the electron-hole wave function overlap is significantly improved to $\Gamma_{e\_hh}=74.83\%$ by the use of AlN-delta-GaN, attributed to the introduction of the delta-GaN layer, which introduces local minima to the QW center. Consequently, a large spontaneous emission rate can be expected for the AlN-delta-GaN QW structure.

The corresponding calculated spontaneous emission spectra for the AlN-delta-GaN QW are plotted in Figure 2(a) with $n=5\times10^{18}\,cm^{-3}$ at 300 K for both TE- and TM-polarizations. As a result, a large TE-polarized spontaneous emission rate is observed with an emission wavelength of 298 nm for the proposed QW structure due to the dominant

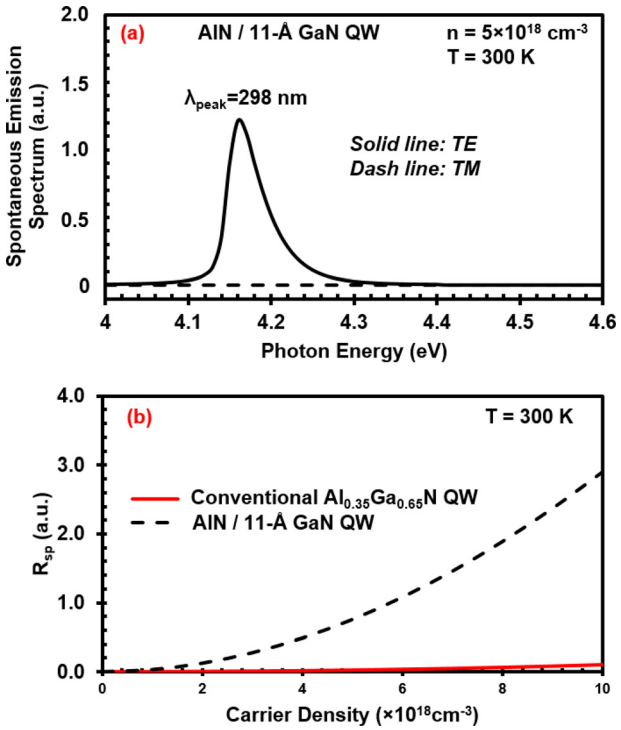

FIG. 2. (a) TE-polarized (solid line) and TM-polarized (dash line) spontaneous emission spectra of the AlN-delta-GaN QW with the 11-Å GaN delta layer at $n = 5 \times 10^{18}\,cm^{-3}$. (b) Spontaneous emission radiative recombination rate (R_{sp}) as a function of carrier density up to $1 \times 10^{19}\,cm^{-3}$ for both the AlN-delta-GaN QW and 30-Å conventional $Al_{0.35}Ga_{0.65}N$ QW.

C-HH transition. Note that the peak emission wavelength can be tuned by adjusting the delta-GaN thickness. Specifically, the use of thicker delta-GaN layers will lead to longer peak emission wavelengths, similar to the finding from Ref. 23.

Figure 2(b) shows the spontaneous emission radiative recombination rate per volume (R_{sp}) for both the AlN-delta-GaN QW and the conventional $Al_{0.35}Ga_{0.65}N$ QW as a function of carrier density up to $1 \times 10^{19}\,cm^{-3}$. For the conventional $Al_{0.35}Ga_{0.65}N$ QW, a significantly lower TE-polarized spontaneous emission rate is predicted because of the much smaller electron-hole wave function overlap. In contrast, the insertion of delta-GaN in the AlN-delta-GaN QW results in a significant improvement of electron and hole wave function overlap and sequentially leads to the increase in the TE-polarized spontaneous emission rate up to 30 times as compared to that of the conventional $Al_{0.35}Ga_{0.65}N$ QW, which again demonstrates that the use of the AlN-delta-GaN QW is promising for the mid-UV regime.

To confirm the polarization properties of the proposed AlN-delta-GaN QW structure, polarization-dependent electroluminescence (EL) measurements were employed in this study to characterize an AlN/GaN QW-like UV LED as indicated in Fig. 3. The LED sample was grown by plasma-assisted MBE on an AlN template on a sapphire substrate with a dislocation density of $\sim 1 \times 10^{10}\,cm^{-2}$. For the active region, an 8-period AlN/GaN QW-like heterostructure was grown and sandwiched between Mg:$Al_{0.5}Ga_{0.5}N$ and Si:$Al_{0.77}Ga_{0.23}N$ cladding layers to have optimal tunnel injection of carriers.[14–16] More details of the epitaxial growth method and device fabrication can be found in Refs. 14–16. The schematic of the AlN/GaN QW-like structure and cross-sectional transmission electron microscopy (TEM) image of the active region are shown in Figure 3. By precise MBE growth control, the thickness of the delta-GaN layer is achieved to be 3–4 monolayers (MLs), while the thickness of the AlN sub-QW layers is ~2.5 nm.

The unpolarized EL spectra and integrated EL intensities were first measured for the AlN-delta-GaN QW LED. The inset of Figure 4 plots the EL spectra of the AlN-delta-GaN QW LED at different injected current densities ($j = 2$–$23\,A/cm^2$). The EL spectra can be further deconvoluted into two independent peaks centered at 298 nm and 308 nm, corresponding to ~2–4 ML delta-GaN thicknesses, respectively. Note that with increased current density, the 298-nm peak becomes more significant, as compared to the peak centered at 308 nm. The broad luminescence spectrum around 300 nm is attributed to the

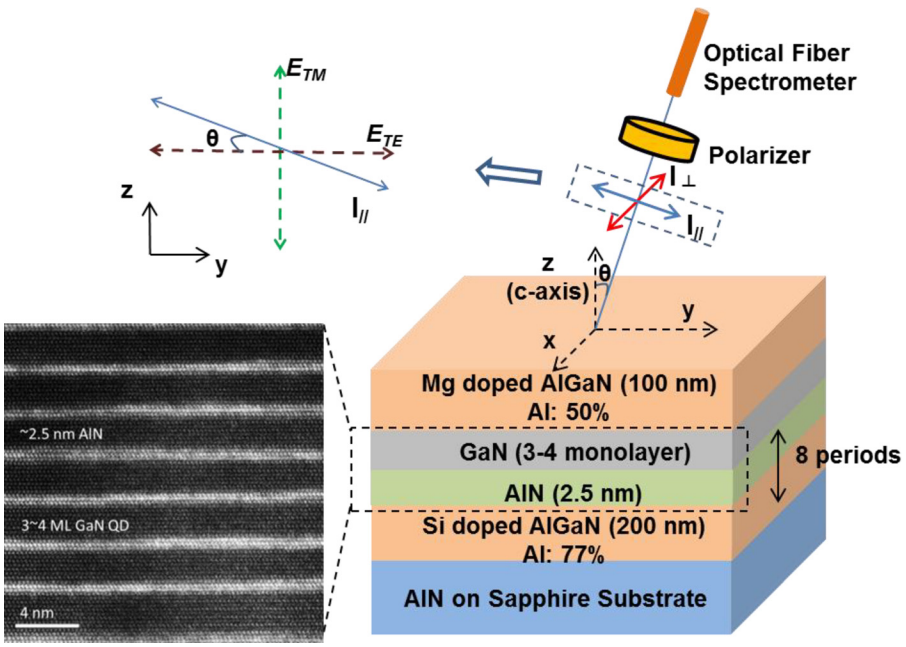

FIG. 3. Schematic diagram of the polarization-dependent EL measurement setup and cross-sectional TEM image of the AlN/GaN QW-like structure, the θ stands for the angle between c-axis and collecting fiber. The polarizer is held on a rotational stage to achieve the intensity in y-z plane ($I_{//}$) and the intensity along x direction ($I_{\perp}$).

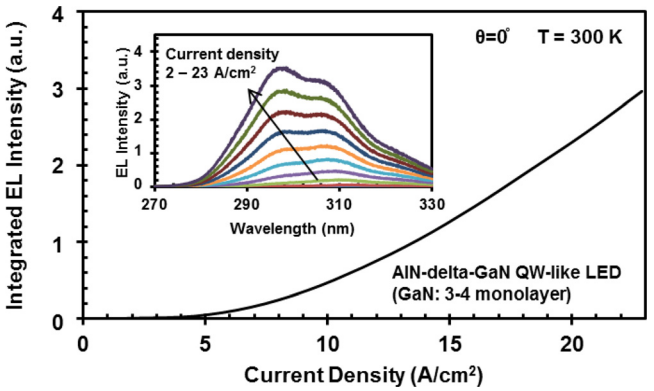

FIG. 4. Integrated EL intensity as a function of current density. Inset: Electroluminescence spectra from the AlN/GaN QW-like LED with different current densities (j = 2–23 A/cm^2).

delta-GaN thickness fluctuation within the range of ~2–4 MLs during the MBE growths, which can be seen from the TEM image in Figure 3. The integrated EL intensities as a function of current injection level are plotted in Figure 4, exhibiting an increasing trend with the increase of carrier injection levels.

The polarization characteristics of the AlN-delta-GaN QW-like UV LED were investigated at room temperature under pulsed current injection with a frequency of 10 kHz and a duty cycle of 5%. The emitted photons are filtered with a Glan-Taylor polarizer and collected by an optical fiber spectrometer. The schematic illustration of polarization-dependent EL measurement setup is shown in Figure 3. Specifically, the LED sample is fixed on a stationary stage while the polarizer and optical fiber are rotated about the x-axis with θ representing the angle between the c-axis and the collecting fiber. The polarizer can also be rotated about the light emitting direction to resolve the $E_{//}$ (electric field in y-z plane) and $E_{\perp}$ (electric field along x-axis). At a particular angle, the corresponding intensities $I_{//}$ and $I_{\perp}$, which are not sole TE and TM components, can be expressed as[2,29,30]

$$I_{//} = I_{TEy}\cos^2\theta + I_{TM}\sin^2\theta, \quad (1)$$

$$I_{\perp} = I_{TEx}, \quad (2)$$

where I_{TM} is the intensity of TM-polarized emission and I_{TEx} and I_{TEy} represent the intensities of TE-polarized emission along x and y directions, respectively. Note that there is no anisotropic emission in the x-y plane; therefore, I_{TEx} and I_{TEy} are identical. For $\theta = 90°$, the measured $I_{//}$ (E // c) and $I_{\perp}$ (E ⊥ c) are identified as TM and TE modes and hence several research groups utilize edge emitted EL measurement to study device polarization properties.

In this study, $I_{//}$ and $I_{\perp}$ are collected at $\theta = 30°$ and $\theta = 45°$ with $\boldsymbol{j} = 40$ A/cm^2. The results plotted in Figure 5 show that $I_{\perp}/I_{//}$ ratios are 1.157 and 1.149 for $\theta = 30°$ and $\theta = 45°$, respectively. Utilizing Equations (1) and (2), the polarization dependent emissions can be determined as $TE_{total} = I_{TEy}\cos^2\theta + I_{TEx}$ and $TM_{total} = I_{TM}\sin^2\theta$. The analysis shows that $TE/TM = 15.3$ when $\theta = 30°$ and $TE/TM = 4.05$ when $\theta = 45°$. In addition, the degree of polarization ($\boldsymbol{P} = (TE-TM)/(TE+TM)$) is also calculated as 0.87 for $\theta = 30°$ and 0.60 for $\theta = 45°$. The positive $\boldsymbol{P}$ values are

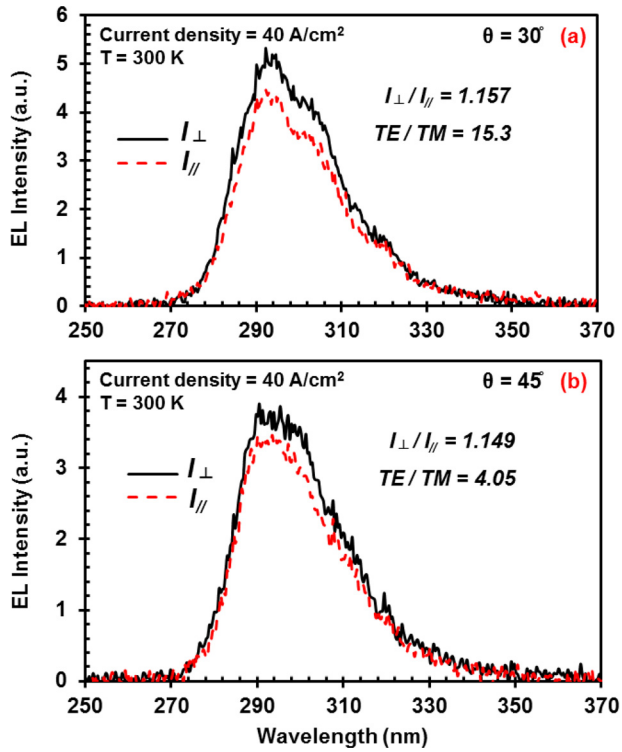

FIG. 5. Polarization-dependent EL spectra from the AlN/GaN QW-like LED at $\theta = 30°$ and $\theta = 45°$ with a current density of 40 A/cm^2.

primarily credited to the dominant TE-polarized spontaneous emission from the active region.

Note that the physics presented in Figure 2 has demonstrated that the dominant TE-polarized emission is attributed to the prevailing C-HH transition and the significant improvement of the electron-HH wave function overlap ($\Gamma_{e\_hh} = 74.83\%$) caused by the insertion of the delta-GaN layer. It is also interesting to note that the larger TM component has been measured with a larger angle (at $\theta = 45°$), which is related to the extraction mechanism of the TM-polarized emission. Therefore, the polarization-dependent measurements of the AlN-delta-GaN QW-like UV LED have confirmed the theoretical prediction and proved the great potential of such a QW structure for high efficiency TE-polarized mid-UV LED application.

As a summary, the physics and polarization properties of photon emission from the proposed AlN-delta-GaN QW were investigated in this study. The use of the delta-GaN layer could strongly improve the electron-hole wave function overlap to 74.83%, which leads to a 30-times enhancement in the TE-polarized spontaneous emission rate as compared to the conventional $Al_{0.35}Ga_{0.65}N$ QW at 298 nm as predicted from the physics model. Polarization-dependent EL measurements were employed in this study to analyze an MBE-grown AlN/GaN QW-like LED, which consists of 3–4 monolayers GaN sandwiched by 2.5-nm AlN sub-QW layers. Note that the η_{EQE} of the AlN-delta-GaN QW LED can be further improved by enhancing the injection efficiency of the device especially from the use of more conductive p-type AlGaN layers. The full width at half maximum (FWHM) from the EL spectra can be narrowed by optimizing the uniformity of the delta-GaN layer, which can be engineered by the MBE growth parameters. In conclusion, the

polarization study confirms the dominant TE-polarized emission with different angles, which indicate the great potential for the AlN-delta-GaN QW structure to serve as a promising candidate for high-efficiency mid-UV emitters.

The authors (C. Liu, Y. K. Ooi, and J. Zhang) would like to acknowledge the support by the Kate Gleason endowed professorship fund from Rochester Institute of Technology and by the Office of Naval Research under Award No. N00014-16-1-2524. The authors (S. M. Islam, J. Verma, H. Xing, and D. Jena) would like to thank the support from the University of Notre Dame and the NSF DMREF program (1534303).

[1]H. Hirayama, N. Maeda, S. Fujikawa, S. Toyoda, and N. Kamata, Jpn. J. Appl. Phys., Part 1 **53**, 100209 (2014).
[2]M. Kneissl and J. Rass, *III-Nitride Ultraviolet Emitters: Technology and Applications*, Springer Series in Material Science Vol. 227 (Springer International Publishing, 2016).
[3]Y. Muramoto, M. Kimura, and S. Nouda, Semicond. Sci. Technol. **29**, 084004 (2014).
[4]M. Kneissl, T. Kolbe, C. Chua, V. Kueller, N. Lobo, J. Stellmach, A. Knauer, H. Rodriguez, S. Einfeldt, Z. Yang, N. M. Johnson, and M. Weyers, Semicond. Sci. Technol. **26**, 014036 (2011).
[5]H. Hirayama, T. Yatabe, N. Noguchi, T. Ohashi, and N. Kamata, Appl. Phys. Lett. **91**, 071901 (2007).
[6]A. Fujioka, T. Misaki, T. Murayama, Y. Narukawa, and T. Mukai, Appl. Phys. Express **3**, 041001 (2010).
[7]W. Sun, M. Shatalov, J. Deng, X. Hu, J. Yang, A. Lunev, Y. Bilenko, M. Shur, and R. Gaska, Appl. Phys. Lett. **96**, 061102 (2010).
[8]F. Mehnke, C. Kuhn, M. Guttmann, C. Reich, T. Kolbe, V. Kueller, A. Knauer, M. Lapeyrade, S. Einfeldt, J. Rass, T. Wernicke, M. Weyers, and M. Kneissl, Appl. Phys. Lett. **105**, 051113 (2014).
[9]F. Mehnke, Ch. Kuhn, J. Stellmach, T. Kolbe, N. Lobo Ploch, J. Rass, M. A. Rothe, Ch. Reich, M. Ledentsov, Jr., M. Pristovsek, T. Wernicke, and M. Kneissl, J. Appl. Phys. **117**, 195704 (2015).
[10]T. Kolbe, F. Mehnke, M. Guttmann, C. Kuhn, J. Rass, T. Wernicke, and M. Kneissl, Appl. Phys. Lett. **103**, 031109 (2013).
[11]Z. Ren, Q. Sun, S. Y. Kwon, J. Han, K. Davitt, Y. K. Song, A. V. Nurmikko, H. K. Cho, W. Liu, J. A. Smart, and L. J. Schowalter, Appl. Phys. Lett. **91**, 051116 (2007).
[12]M. Jo, N. Maeda, and H. Hirayama, Appl. Phys. Express **9**, 012102 (2016).
[13]Y. Zhang, A. A. Allerman, S. Krishnamoorthy, F. Akyol, M. W. Moseley, A. M. Armstrong, and S. Rajan, Appl. Phys. Express **9**, 052102 (2016).
[14]J. Verma, S. M. Islam, V. Protasenko, P. K. Kandaswamy, H. Xing, and D. Jena, Appl. Phys. Lett. **104**, 021105 (2014).
[15]S. M. Islam, V. Protasenko, S. Rouvimov, H. Xing, and D. Jena, Jpn. J. Appl. Phys., Part 1 **55**, 05FF06 (2016).
[16]J. Verma, P. Kandaswamy, V. Protasenko, A. Verma, H. Xing, and D. Jena, Appl. Phys. Lett. **102**, 041103 (2013).
[17]J. Simon, V. Protasenko, C. Lian, H. Xing, and D. Jena, Science **327**, 60 (2010).
[18]J. Zhang, H. Zhao, and N. Tansu, Appl. Phys. Lett. **97**, 111105 (2010).
[19]T. Kolbe, A. Knauer, C. Chua, Z. Yang, H. Rodrigues, S. Einfeldt, P. Vogt, N. M. Johnson, M. Weyers, and M. Kneissl, Appl. Phys. Lett. **97**, 171105 (2010).
[20]X. H. Li, T. T. Kao, M. M. Satter, Y. O. Wei, S. Wang, H. Xie, S. C. Shen, P. D. Yoder, A. M. Fischer, F. A. Ponce, T. Detchprohm, and R. D. Dupuis, Appl. Phys. Lett. **106**, 041115 (2015).
[21]J. E. Northrup, C. L. Chua, Z. Yang, T. Wunderer, M. Kneissl, N. M. Johnson, and T. Kolbe, Appl. Phys. Lett. **100**, 021101 (2012).
[22]C. Reich, M. Guttmann, M. Feneberg, T. Wernicke, F. Mehnke, C. Kuhn, H. Rass, M. Lapeyrade, S. Einfeldt, A. Knauer, V. Kuller, M. Weyers, R. Goldhahn, and M. Kneissl, Appl. Phys. Lett. **107**, 142101 (2015).
[23]J. Zhang, H. Zhao, and N. Tansu, Appl. Phys. Lett. **98**, 171111 (2011).
[24]Y. Taniyasu and M. Kasu, Appl. Phys. Lett. **99**, 251112 (2011).
[25]H. Zhao, R. A. Arif, Y. K. Ee, and N. Tansu, IEEE J. Quantum Electron. **45**, 66 (2009).
[26]H. Zhao, G. Liu, and N. Tansu, Appl. Phys. Lett. **97**, 131114 (2010).
[27]C. Liu, Y. K. Ooi, and J. Zhang, J. Appl. Phys. **119**, 083102 (2016).
[28]S. L. Chuang, *Physics of Photonic Devices*, 2nd ed. (Wiley, New York, 2009), Chap. 4.
[29]J. Shakya, K. Knabe, K. H. Kim, J. Li, J. Y. Lin, and H. X. Jiang, Appl. Phys. Lett. **86**, 091107 (2005).
[30]X. Chen, C. Ji, Y. Xiong, X. Kang, B. Shen, and T. Yu, Opt. Express **24**(10), A935 (2016).